

How much can novel solid sorbents reduce the cost of post-combustion CO₂ capture? A techno-economic investigation on the cost limits of pressure-vacuum swing adsorption

Sai Gokul Subraveti^a, Simon Roussanaly^{b,*}, Rahul Anantharaman^b, Luca Riboldi^b, Arvind Rajendran^{a,*}

^a*Department of Chemical and Materials Engineering, University of Alberta, 12th floor, Donadeo Innovation Centre for Engineering (ICE), 9211-116 Street, Edmonton, Alberta T6G1H9, Canada*

^b*SINTEF Energy Research, NO-7465, Trondheim, Norway*

Abstract

This paper focuses on identifying the cost limits of two single-stage pressure-vacuum swing adsorption (PVSA) cycles for post-combustion CO₂ capture if the “ideal” zero-cost adsorbent can be discovered. Through an integrated techno-economic optimisation, we simultaneously optimise the adsorbent properties (adsorption isotherms and particle morphology) and process design variables to determine the lowest possible cost of CO₂ avoided (excluding the CO₂ conditioning, transport and storage) for different industrial flue gas CO₂ compositions and flow rates. The CO₂ avoided cost for PVSA ranges from 87.1 to 10.4 € per tonne of CO₂ avoided, corresponding to CO₂ feed compositions of 3.5 mol% to 30 mol %, respectively. The corresponding costs for a monoethanolamine based absorption process, using heat from a natural gas plant, are 76.8 to 54.8 € per tonne of CO₂ avoided, respectively showing that PVSA can be attractive for flue gas streams with high CO₂ compositions. The “ideal” adsorbents needed to attain the lowest possible CO₂ avoided costs have a range of CO₂ affinities with close to zero N₂ adsorption, demonstrating promise for adsorbent discovery and development. The need for simultaneously optimizing the particle morphology and the process conditions are emphasized.

Keywords: carbon dioxide capture and storage, pressure vacuum swing adsorption, techno-economic analysis, optimisation, metal-organic frameworks

*Corresponding authors

Email addresses: Simon.Roussanaly@sintef.no (Simon Roussanaly),
arvind.rajendran@ualberta.ca (Arvind Rajendran)

1. Introduction

Carbon dioxide capture and storage (CCS) from point sources are expected to play a key role in decarbonising the global energy and industry sectors[1, 2]. The feasibility of implementing CCS may vary from one industry to the other since several factors such as CO₂ composition, pressure, the flow rate of the flue gas, system-level integration aspects etc. affect the attractiveness of CCS [3]. In the context of system-level integration, post-combustion CO₂ capture can be retrofitted into existing chemical/power plants in a rather straightforward manner without restructuring the plant layout and has been identified as one of the viable technologies in short- to medium-term [4]. While the majority of industrial sources emit CO₂ containing gases at atmospheric pressure, the variation in CO₂ composition is typically in the range of 3.5-30% across industries [5]. Although there are several CO₂ capture technologies considered for post-combustion CO₂ capture, the associated energy penalty and cost expenditure remains a barrier for the large-scale implementation [6]. Among all, solvent-based CO₂ capture is at the forefront owing to its technological maturity and commercial implementation. Adsorption-based processes are proposed as an alternative to the traditional solvents for their ability to lower the energy penalty and the costs related to the capture [6].

One of the main drivers determining the performance of adsorption processes is the choice of adsorbents. Recent developments in material science have facilitated material chemists to discover several new classes of adsorbents, such as metal-organic frameworks (MOFs), covalent-organic frameworks (COFs), etc., that can be highly tuned for CO₂ capture applications [4]. Since each class can typically consist of hundreds of thousands of materials, including both real and hypothetical structures, the selection of suitable adsorbents remains crucial for assessing the potential of adsorptive CO₂ capture. The quest for the best performing adsorbents has resulted in several *in-silico* material screening studies that use various performance metrics to rank materials [7, 8, 9, 10, 11, 12, 13, 14, 15, 16]. While the initial focus primarily relied on simplified process metrics (derived under equilibrium conditions) as means to evaluate the performance of adsorbents in the real process, integration of dynamic process modelling and optimisation into adsorbent screening was later identified as a reliable tool to evaluate the realistic performance of adsorbents [12, 10, 13, 17, 18, 16, 19]. As a result, studies focusing on the *multiscale screening* of known material databases have emerged wherein the adsorbent properties determined through molecular simulations are later incorporated into the process simulation and optimisation routines to identify/rank top material performers based on key process-oriented metrics such as the CO₂ purity, CO₂ recovery, energy penalty, productivity or cost of the CO₂ capture [18, 13, 17, 16]. Alternatively, the problem of identifying the desirable adsorbent properties in processes was also approached through *process inversion* [20, 21]. The *process inversion* approach focuses on determining the “ideal” adsorbent properties that result in the best process performance through an integrated adsorbent-process optimisation. In other words, the adsorbent properties are simultaneously optimised along with the process variables in the optimisation. This approach

helps in identifying the best performance limits of adsorptive CO₂ capture [20]. Both simplified and detailed process models have been used in this approach. For instance, feature spaces of adsorbent properties such as CO₂ and N₂ adsorption isotherms, heat of adsorption, Henry’s constant, etc., were probed using *process inversion* approach in order to determine the lowest energy penalty [22, 20, 23] and CO₂ capture costs [21, 15] for post-combustion adsorptive CO₂ capture. More recently, Pai *et al.* explored adsorbent properties such CO₂ and N₂ adsorption equilibria that minimise the energy penalty and maximise the productivity for different flue gas compositions using a machine learning model [24].

In our earlier publication[25], we demonstrated that the realistic performance of adsorbents should be assessed by incorporating a comprehensive techno-economic analysis framework with detailed process modelling and optimisation. This is primarily because the cost assessment captures the inherent complexities associated with the scale-up of the processes for industrial applications, which otherwise are not quantified when using process performance metrics such as energy penalty or productivity.

While previous studies provide some insights into understanding the underlying relationships between the adsorbent properties and the process performance, in this study, we pose the following key questions:

1. If “ideal” adsorbent(s) were discovered, what are the cost limits of adsorptive post-combustion CO₂ capture from industrial flue gases?
2. How do the costs compare with the benchmark technology, i.e. absorption?

Addressing these questions is critical to understand the true potential of adsorption processes and thus allow for advances in both material discovery and process design. This paper aims to answer the questions mentioned above by employing a *process inversion* approach. We restrict our analysis to single-stage pressure-vacuum swing adsorption (PVSA) technology, a widely studied class of adsorption processes for CO₂ capture applications. In this study, we define the cost limits as the lowest possible achievable costs for capturing CO₂ from post-combustion industrial flue gases using “ideally” desired adsorbent features in the PVSA process considered. Moreover, we also use this opportunity to show the impact of parameters such as the vacuum level required in the process, pellet morphology and adsorbent costs on PVSA costs. Further, we carry out a one-to-one comparison with benchmark monoethanolamine (MEA) solvent cases for various industrial applications. Finally, the cost performance of two “real” adsorbents are evaluated and compared with the limits to identify the potential for “*material innovation*”. This is the first study to report such a comprehensive analysis to the best of the authors’ knowledge.

The current article is organised as follows: the next section summarises the different cases we considered to encompass the wide range of industrial applications. In the computational details section, the *process inversion* approach through integrated techno-economic optimisation framework is explained, and details of adsorbent properties, process model, scale-up and economic assessment are provided. The results and discussion section reports the findings obtained from optimisations and compares them with benchmark MEA-based CO₂ capture case. The merits and demerits of PVSA for post-combustion CO₂ capture are discussed in the concluding remarks, along with some perspectives towards the advancement

of adsorptive CO₂ capture.

2. Case study

For this study, a case matrix comprising a wide range of CO₂ compositions at different flue gas flow rates is considered to represent various industrial post-combustion flue gas sources adequately [5]. Under dry conditions, the flue gas consists of CO₂/N₂ binary mixture and the CO₂ molar compositions in the flue gas are varied between 3.5% and 30%. This range corresponds to flue gas sources from simple cycle gas turbine plants, natural gas combined cycle power plants, coal-fired power plants, cement and steel industries. Further, the analysis is extended to different flue gas flow rates ranging from 303 tonnes/h to 3696 tonnes/h to account for the effect of the scale of operation. Table 1 illustrates the case matrix used in this study. In all cases, the flue gas is available at 1 bar and 35 °C for post-combustion CO₂ capture.

The system under consideration includes CO₂ capture from dry flue gas. We exclude the following while estimating the costs: the process that emits CO₂ containing flue gas, CO₂ conditioning, CO₂ transport and CO₂ storage. The process layout of adsorptive CO₂ capture is provided in Fig. S1 in the supporting information. The dry flue gas further undergoes compression followed by cooling to 25 °C. Multiple adsorption process trains with each N columns are employed to treat the dry flue gas. The CO₂ rich product and N₂ are collected separately using separate vacuum pumps.

Further, adsorptive CO₂ capture is benchmarked against the baseline monoethanolamine-based (MEA) technology to fully understand the potential of adsorption process technology for various industrial applications. To be consistent, the system boundaries for both PVSA- and MEA-based CO₂ capture were kept the same. The MEA-based CO₂ capture performances based on Fu et al [5] are summarised in the supporting information.

Table 1: Case matrix related to different CO₂ compositions and flue gas flow rates considered in this study. Industrial examples are also highlighted where vertical text was used to represent specific industrial cases that have similar flow rates as considered in this study, while the horizontal text was used to indicate industrial examples with similar CO₂ compositions.

| CO ₂ composition (%) | Flue gas flow rate (tonne h ⁻¹) | | | | | |
|---------------------------------|---|------------------------|------|------|-----------------------------|--|
| | 313 | 1159 | 2004 | 2850 | 3696 | |
| 3.5 | 32 MW offshore gas turbine | Gas turbine | | | 1000 MW coal power plant | |
| 7.5 | | | | | | |
| 13 | | Coal-fired power plant | | | | |
| 20 | | Cement | | | | |
| 30 | | Steel | | | | |

3. Computational details

The cost limits of adsorptive CO₂/N₂ binary mixture separations are determined using a recently developed integrated techno-economic optimisation model [25]. Our computational framework integrates adsorbent, process and economic aspects to determine the cost-optimal performance of adsorptive post-combustion CO₂ capture on industrial scales, as shown in Fig. S2 in the supporting information. Both adsorbent properties and process design parameters are simultaneously optimised herein to determine the lowest possible costs.

3.1. Adsorbent features

Adsorbent properties that are required for process modelling include CO₂ and N₂ adsorption isotherms, crystal density, isosteric heats of adsorption, pellet porosity, pellet diameter and specific heat capacity. Physicochemical properties such as CO₂ and N₂ adsorption isotherms, crystal density and isosteric heats of adsorption are inherent crystal properties, while pellet porosity, pellet diameter and specific heat capacity are properties of adsorbent within the adsorption column.

A practically deployable sorbent for CO₂ capture should have several critical features, e.g., low cost, scalability, stability, etc. However, the ability to separate CO₂ and N₂, i.e., the two key components of flue gas, is arguably the most important feature. Most practical adsorption-based CO₂ and N₂ separations exploit the differences in affinity between CO₂ and N₂ on a specific sorbent. The affinity is expressed in the form of an adsorption isotherm that relates the fluid and solid phase concentrations at equilibrium. The hypothetical CO₂ and N₂ adsorption isotherms were expressed in terms of the competitive dual-site Langmuir (DSL) isotherm model. The advantages of using the competitive DSL isotherm model involve computational simplicity (because of the explicit formulation), and also the ability to adequately represent the mixture equilibrium predictions from single component parameters for many practical systems [26, 10]. The competitive DSL isotherm model (for component i) is given by,

$$q_i^* = \frac{q_{sb,i} b_i c_i}{1 + \sum_i b_i c_i} + \frac{q_{sd,i} d_i c_i}{1 + \sum_i d_i c_i} \quad i = \text{CO}_2, \text{N}_2 \quad (1)$$

In Eq. 1, c_i is the fluid phase concentration of component i , q_i^* is the equilibrium solid-phase loading of the component i , $q_{sb,i}$ and $q_{sd,i}$ represent saturation capacities for the two sites and, b_i and d_i are the temperature dependent adsorption equilibrium constants defined as:

$$b_i = b_{0,i} e^{\left(-\frac{\Delta U_{b,i}}{RT}\right)} \quad (2a)$$

$$d_i = d_{0,i} e^{\left(-\frac{\Delta U_{d,i}}{RT}\right)} \quad (2b)$$

where $\Delta U_{b,i}$ and $\Delta U_{d,i}$ are the internal energies of the two sites.

3.2. Process model and economic analysis

Two pressure-vacuum swing adsorption (PVSA) cycles are considered in this work. The first cycle illustrated in Fig. S3 (in the supporting information) consists of four steps:

1. Adsorption step (ADS): Feed mixture introduced in the column for a duration of t_{ADS} at high pressure (P_{H}) undergoes separation through preferential adsorption of the heavy component CO_2 while light component N_2 leaves the column.
2. Blowdown step (BLO): Co-current blowdown to an intermediate vacuum (P_{I}) to remove N_2 from the column. If $P_{\text{H}} > 1$ bar, then the column pressure first reduces to atmospheric pressure using a valve and further down to P_{I} using a vacuum pump. If $P_{\text{H}} = 1$ bar, then only vacuum pump reduces the column pressure to P_{I} .
3. Evacuation step (EVAC): Column pressure further reduced to a low vacuum (P_{L}) using a vacuum pump in the counter-current direction to collect CO_2 rich product at the feed end of the column.
4. Light product pressurisation step (LPP): Light product from the adsorption column pressurises the column back to high pressure.

Owing to its simple features, this cycle has been benchmarked by various studies [21, 20, 18, 16] and was also demonstrated at a pilot plant facility [27]. We considered a more complex six-step PVSA cycle with dual reflux (DR) as the second cycle [28, 20, 21]. The cycle schematic is shown in Fig. S4 in the supporting information. In addition to the four steps above, this cycle comprises two reflux steps:

5. Light reflux (LR) step after the evacuation at P_{L} where the light product from the adsorption column is used as reflux to purge the column in the LR step.
6. Heavy reflux (HR) step after the adsorption step at P_{H} by using the product from the LR step in order to increase the CO_2 partial pressure in the column.

The process simulations were carried out using a non-isothermal, one-dimensional mathematical model obtained by solving mass, momentum and energy balances [29]. The model comprises a set of partial differential equations (PDEs) after incorporating the following assumptions: 1) gas-phase obeys ideal gas law, 2) axially dispersed plug flow represents the bulk flow, 3) linear driving force model characterises the solid phase mass transfer, 4) there exist no radial gradients for composition, pressure and temperature across the column, 5) Ergun's equation accounts for the pressure drop across the column, 6) adsorbent properties and bed porosity are uniform, 7) the process operation remains adiabatic and, 8) instantaneous thermal equilibrium exists between the gas and the solid. More details on the PVSA model equations, appropriate boundary conditions used for each step in the cycle and the simulation parameters can be found in the supporting information. The PDEs were numerically discretised into 30 finite volumes along the spatial domain using the finite volume method with a weighted essentially non-oscillatory (WENO) scheme [29]. The resulting ordinary differential equations (ODEs) were then integrated using *ode23tb* [30], a stiff ODE solver in MATLAB. The cycle simulations were carried out based on a standard uni-bed approach where a single column undergoes all cycle steps in a sequence. The column was

initialised with a feed mixture at P_L and simulated until the process reached cyclic steady state (CSS). When the mass balance error for the PVSA process equals 1% or less was observed for five consecutive cycles, the process was considered to attain CSS. A minimum number of 50 cycles were simulated to ensure that the CSS criterion was adequate. For simulations where the system fails to achieve CSS, a maximum number of 500 cycles were simulated, after which it was assumed that the system attained CSS. At CSS, state variables such as composition, pressure and temperature profiles were determined to calculate key performance indicators. The process model was previously demonstrated to reproduce both lab-scale and pilot-scale experiments [31, 27].

The column scheduling was carried out based on the method proposed by Khurana and Farooq [21] to determine the number of columns required for continuous operation. The main assumptions are reiterated as follows: 1) Continuous-feed operation with constant throughput, 2) Separate vacuum pumps used to collect CO_2 and N_2 from respective steps to avoid contamination, 3) One vacuum pump serves only one column at any given time and, 4) Coupled steps occur simultaneously to avoid using storage tanks. More details on the column scheduling are provided in the supporting information. The modelling of a vacuum pump performance plays a crucial role in process simulations. Two key approaches, already used in our previous work [25], are incorporated here. First, the flow rate of the vacuum pump is incorporated as the boundary condition. This provides a realistic estimation of blowdown and evacuation times. Second, the efficiency of the vacuum pump is made a function of the pressure, i.e., the vacuum pump efficiency drops as per the expression provided in the supporting information. This ensures a realistic estimation of the power consumption.

The economic analysis was carried out based on the cost model developed in a previous study [25] and the cost assessment was performed on an aspirational Nth Of A Kind (NOAK) basis [32] wherein it was assumed that the adsorptive CO_2 capture is mature for commercial deployment. This is the state-of-the-art approach used and recommended by organisations like NETL and IEAGHG to estimate the potential cost of an advanced technology for the optimistic case in which all R&D goals and assumptions are realized at some point in the future [32]. The cost estimates are provided in €_{2016} price levels. Costs with older estimates were updated using Chemical Engineering Plant Cost Index (CEPCI) and inflation. More details on the cost model are provided in the supporting information. While undertaking techno-economic analyses, the outcomes can significantly change depending on the assumptions and the design choices. [33] Hence, we note that the techno-economic model used in this study obeys both technical and economic recommendations for adsorption processes [33] and are consistent with best practices [32].

3.3. Integrated techno-economic optimisation

Integrated techno-economic optimisation problem was formulated to minimize the CO_2 avoided cost of the PVSA technology while achieving a minimum of 95% CO_2 purity and 90% CO_2 recovery. To this end, both process and adsorbent design variables were used as decision variables in the optimisation problem.

Process decision variables: adsorption step duration (t_{ADS}), high pressure (P_H), intermediate vacuum (P_I), low vacuum (P_L), column length (L), reflux fraction (θ_R), fractional

duration of reflux steps (f_t), volumetric flow rates of blowdown (S_B) and evacuation (S_E) vacuum pumps.

Adsorbent decision variables: CO₂ DSL isotherm parameters (q_{sb,CO_2} , q_{sd,CO_2} , $\Delta U_{b,CO_2}$, $\Delta U_{d,CO_2}$, b_{0,CO_2} , d_{0,CO_2}), N₂ DSL isotherm parameters ($\Delta U_{b,N_2}$, b_{0,N_2}), pellet porosity (ϵ_p) and pellet diameter (d_p).

Most of the process decision variables were kept the same as that of the previous study [25]. Additionally, the high pressure (P_H) in the adsorption step was also varied. Although feed velocity in the adsorption step can be explicitly varied in the optimisation, it was not considered as a decision variable in the present work. This was because the optimiser in an earlier study always approached the upper bounds in the techno-economic optimisations in order to reduce the total number of trains required for the separation [25]. Hence, in the current study, the feed velocity was calculated as the minimum fluidisation velocity which is the maximum velocity at which the packed beds can operate theoretically. Since the fluidisation velocity depends on the decision variables P_H , ϵ_p and d_p , feed velocity can be considered as a dependent variable. Reflux fraction (θ_R) was defined as the fraction of the adsorption outlet flow that goes as the feed to the LR step in the six step DR cycle while the fractional duration of LR and HR steps relate to the LR and HR step durations as: $t_i = f_t t_{ADS}$, where $i = HR, LR$. The length to diameter ratio of the adsorption columns was fixed to 3.

Different hypothetical CO₂ and N₂ adsorption isotherms can be generated by varying the parameters q_{sb} , q_{sd} , b_0 , d_0 , ΔU_b and ΔU_d . For many known adsorbents, CO₂ adsorption is heterogeneous and the DSL isotherm model can reasonably describe the equilibrium while N₂ adsorption is homogeneous [20]. Consequently, the DSL isotherm parameter variation was constrained such that both thermodynamic consistency and homogeneity of N₂ adsorption are maintained. This can be accomplished by describing the competition between CO₂ and N₂ between the two sites using equal energy site (EES) formulation [18]. Here, the saturation capacity of each site remains the same for both components, i.e., $q_{sb,CO_2} = q_{sb,N_2}$ and $q_{sd,CO_2} = q_{sd,N_2}$. Also, the internal energy of adsorption and constants b_0 and d_0 for N₂ are kept identical between the two sites, i.e., $\Delta U_{b,N_2} = \Delta U_{d,N_2}$ and $b_{0,N_2} = d_{0,N_2}$. Experimental evidence also supported this type of formalism for Zeolite 13X [31]. The physicochemical properties for achieving lowest costs are examined by considering the following parameters q_{sb,CO_2} , q_{sd,CO_2} , $\Delta U_{b,CO_2}$, $\Delta U_{d,CO_2}$, b_{0,CO_2} , d_{0,CO_2} , $\Delta U_{b,N_2}$, b_{0,N_2} . In a recent study, Farhamini *et al* [16] showed that both pellet porosity (ϵ_p) and pellet diameter (d_p) can significantly affect the process performance. Hence, the variation of ϵ_p and d_p was also considered in the optimisation. Other properties such as crystal density and the specific heat capacity of the adsorbent are held constant to that of Zeolite 13X. While specific heat capacity can potentially impact the process performance,[16] especially under adiabatic conditions, it is, however, held constant because of lack of data. It is also worth noting that a wide range of parametric space of the adsorbent properties is defined so that the properties of actual adsorbents, real or hypothetical, will only be a subset of what is considered in the study.

The lower and upper bounds defined for the decision variables are provided in Table S12 in the supporting information. A global search method, non-dominated sorting genetic

algorithm II (NSGA-II), was used to solve the constrained optimisation problem in MATLAB 2018b. The constraints were handled as penalty terms in the objective function. The initial set of decision variables were generated using Latin hypercube sampling and at least 20000 NSGA-II evaluations were carried out in each optimisation to ensure that the solution has converged. For convergence, we also ensured that the average relative tolerance is less than 0.001.

4. Results and Discussion

4.1. Cost limits of four-step PVSA cycle

Unique optimisations were carried out to determine the minimum CO₂ avoided cost for each of the cases specified in Table 1. The optimisation was performed by varying both adsorbent and process design variables simultaneously in the optimisations. Note that the requirements of minimum 95% CO₂ purity and 90% CO₂ recovery were considered as constraints for all optimisations in this paper. The costs of adsorbents have been set to zero in these optimisations, which were based on the assumption that the “ideal” hypothetical adsorbent(s) identified using *process inversion* can be synthesised or available for zero-cost. Although not plausible practically, this assumption will determine the absolute minimum costs of building and operating simply the PVSA process alone without additional expenditures related to the adsorbent.

Figure 1 (a) illustrates the minimum CO₂ avoided costs (or the cost limits) obtained over a range of CO₂ compositions for a flue gas flow rate of 2004 tonnes h⁻¹ at atmospheric pressure. The CO₂ avoided costs increase with decrease in CO₂ compositions. For instance, the minimum CO₂ avoided cost obtained for 30% CO₂ composition is 12.2 € per tonne of CO₂ avoided and the CO₂ avoided cost increases 1135% when the CO₂ composition is reduced from 30% to 3.5%. In Fig. 1(c) and (e), we show the breakdown of the capital and operating costs that add up to the minimum CO₂ avoided costs. Note that the individual cost breakdown of capital and operating costs along with optimal decision variables for all optimisations reported in this study are tabulated in Tables S13-S20 in the supporting information. As can be observed from Figs. 1(c) and (e), the capital costs contribute to about 24-32% of the avoided costs over a range of CO₂ compositions, and operating costs drive the techno-economic of PVSA. The operating costs amount to about 68% of the total costs for the case of 30% CO₂ composition, and this relative contribution increases to about 76% when the CO₂ composition is reduced to 3.5%. The major contribution to operating costs comes from the electricity consumption, which varies between 77% and 84% of the operating costs. The electricity requirements costs 6.4 € per tonne of CO₂ avoided for 30% CO₂ composition case, however, when the CO₂ composition is reduced to 3.5%, the electricity costs escalate to 95.5 € per tonne of CO₂ avoided. Such high electricity demands with the decrease in CO₂ composition can be attributed to the P_H and P_L required in the process and due to low efficiency of the vacuum pumps at low pressures.

Figure 2 shows the optimal values of P_H and P_L obtained over a range of CO₂ compositions. The shaded region around the optimal values represent the upper and lower limits of the solutions obtained within the 5% vicinity of the minimum CO₂ avoided costs. The

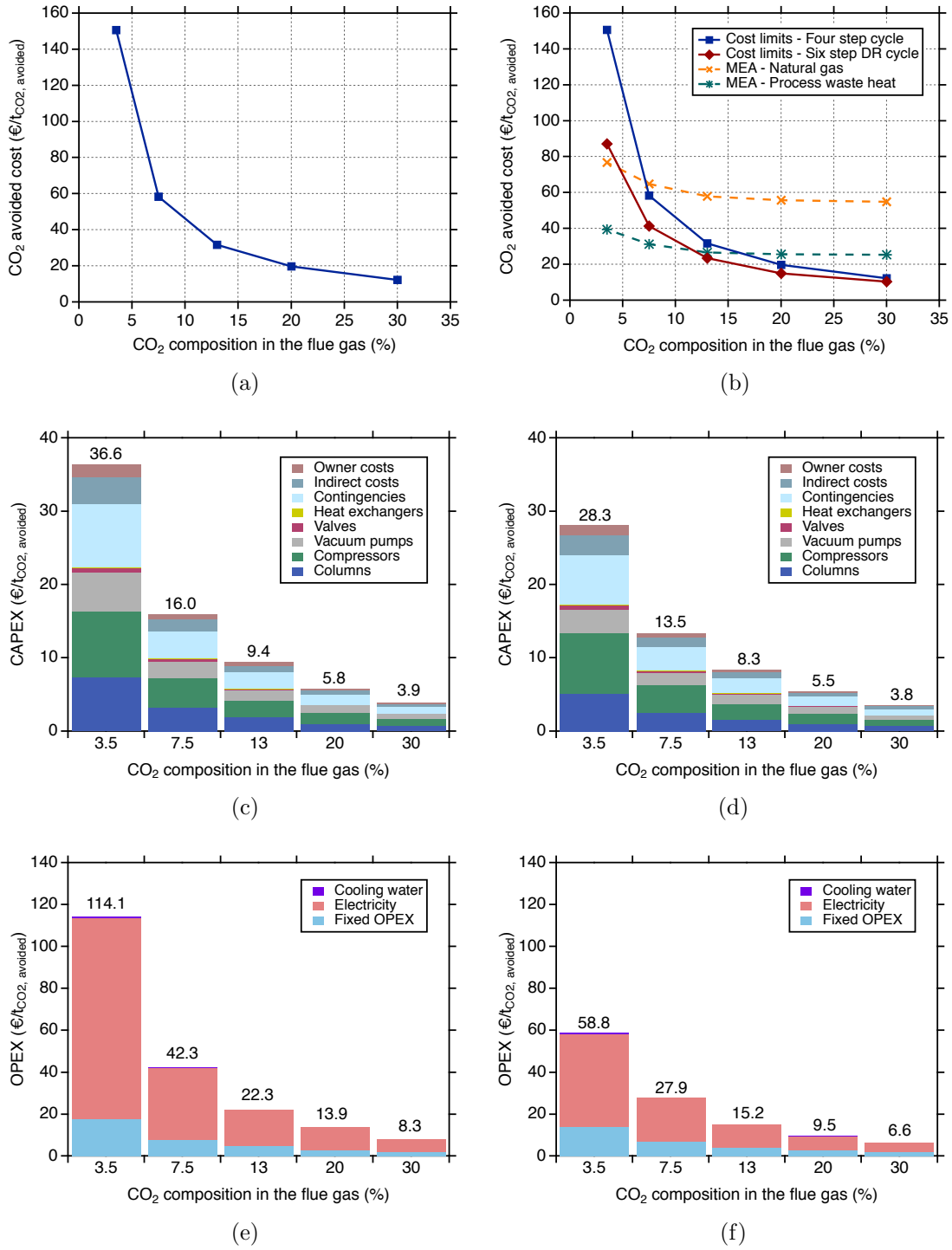


Figure 1: (a) Cost limits (or the lowest possible CO₂ avoided costs) of the four-step PVSA cycle at different CO₂ compositions. (b) Comparison between the cost limits of both four-step and six-step DR PVSA cycles with CO₂ avoided costs obtained using the MEA-based CO₂ capture with two steam supply scenarios (natural gas boiler and waste heat recovery). CO₂ avoided costs reported here exclude CO₂ conditioning, transport and storage. (c) Breakdown of investment costs (CAPEX) related to the cost limits of the four-step cycle. (d) Breakdown of investment costs (CAPEX) related to the cost limits of the six-step DR cycle. (e) Breakdown of operating costs (OPEX) related to the cost limits of the four-step cycle. (f) Breakdown of operating costs (OPEX) related to the cost limits of the six-step DR cycle.

rationale behind this is to account for the variation of P_H and P_L on the minimum avoided cost. As expected, P_L decreases from ≈ 0.11 bar to 0.01 bar with lowering CO_2 composition from 30% to 3.5%, respectively; contrarily, P_H increases from 1.8 bar to 2.9 bar. This trend is observed because the process requires a certain amount of working capacity from the adsorbent to meet the 95% CO_2 purity and 90% CO_2 recovery constraints. Hence, a higher pressure ratio, P_H/P_L is required.

We now turn our attention to the adsorbent properties that link to the cost limits. Figures 3(a)-(f) show the optimal (or “ideal”) single component CO_2 and N_2 isotherms for different CO_2 compositions. The CO_2 isotherms of the ideal adsorbent (shown in red) indicate that they are all quite linear for all CO_2 compositions. The corresponding N_2 isotherms invariably converged close to zero loading. When we analysed the solutions near the minimum cost value for each case, we found that more than one CO_2 isotherm resulted in similar CO_2 avoided costs. Hence, in addition to the optimal CO_2 isotherms, we have included all the corresponding CO_2 isotherms obtained within the vicinity of 5% of the minimum CO_2 avoided costs. These CO_2 isotherms are illustrated as Box and Whisker plots in Figs. 3(a)-(e) to statistically represent the entire region of distribution along with minimum and maximum values. As can be seen from Figs. 3(a)-(e), there is a wide range of CO_2 isotherms resulting in similar cost performance. As illustrated in the figure, this band of CO_2 isotherms is generally closer to being linear with varied adsorption capacities. It is worth noting that the box and whisker plots are obtained from CO_2 isotherms which were evaluated as a part of the optimisation algorithm. Hence, these should be viewed as a subset of all possible isotherms that would yield cost values within 5% of the minimum value. The goal here was not to find the entire range but to highlight how widely varying CO_2 isotherms can indeed result in similar costs. Such a wide range CO_2 adsorption capacities can be attributed to trade-offs between competing capital and electricity expenditure towards overall CO_2 avoided costs. This is a key observation that points to the possibility that multiple adsorbents may be able to provide the comparable (low) cost of CO_2 capture. However, they may display widely varying CO_2 isotherms. This also highlights why the interplay between material property and process performance should be studied together. The optimal N_2 isotherms are shown in Fig. 3(f). Since the N_2 affinity for all cases was almost zero, the isotherms around the optimum were not considered. This again confirms that low N_2 adsorption is a very desirable property of an ideal adsorbent. Moreover, we have also considered a $\pm 10\%$ variation in optimal adsorbent variables to find out the uncertainty of optimal adsorbent variables on the cost limits of four-step PVSA cycle for 20% CO_2 composition illustrated in Fig. 1(a). To this end, the influence of uncertainty of adsorbent properties on the cost limits is illustrated in Fig. S8 in the supporting information.

Limiting P_L to 0.1 bar.. One of the challenges of large-scale implementation of PVSA involves deep vacuum ($P_L < 0.1$ bar) requirements to achieve very high CO_2 purity-recovery targets. Acknowledging the practical limitations to implement deep vacuum in industrial applications, we increased the lower limit of P_L in the optimisations from 0.01 bar to 0.1 bar and investigated the impact on cost limits. After running unique optimisations for the case of the lower limit of $P_L = 0.1$ bar, we then compared the obtained cost limits to the previous

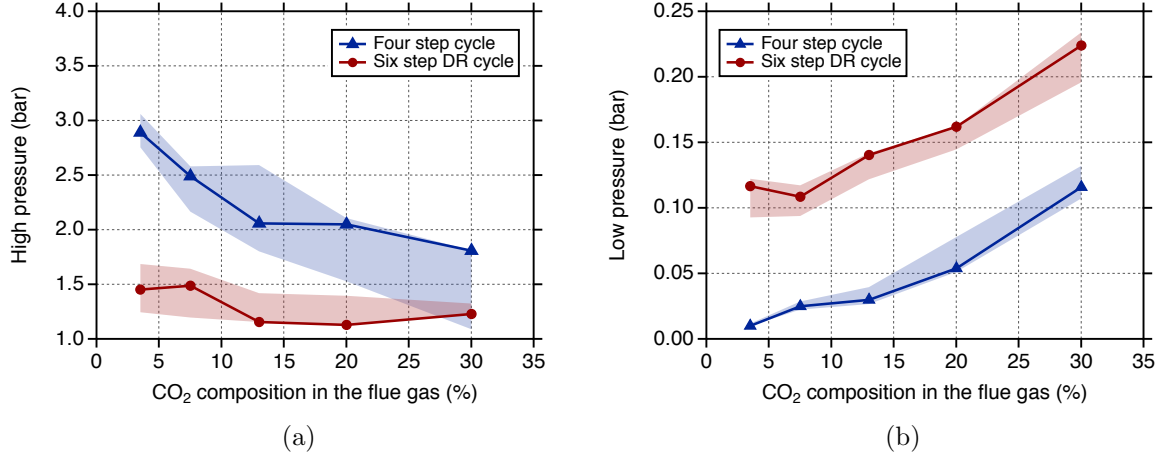


Figure 2: Optimal high pressures (P_H) and low pressures (P_L) corresponding to the cost limits obtained at different CO₂ compositions. Shaded region represents the range of P_H and P_L within the 5% vicinity of the lowest possible CO₂ avoided costs.

case. Figure 4(a) illustrates the ratio of cost limits obtained in both cases at different CO₂ compositions. For 3.5% and 7.5% CO₂ compositions, CO₂ purity-recovery constraints were not met in the optimisations and hence, we did not consider these compositions for the discussion. The cost limits decreased with an increase in CO₂ compositions. The difference between two cases remains minor ($\leq 6\%$) for CO₂ compositions from 20% to 30% while at 13% CO₂ composition, a difference of 14% was observed. This indicates that the four-step PVSA process can still be operated at higher P_L (≥ 0.1 bar) for higher CO₂ compositions but requires ultra-deep vacuum for lower CO₂ compositions in order to meet purity-recovery requirements.

Effect of pellet porosity and pellet size.. One set of adsorbent decision variables in the cost limit optimisations relate to adsorbent properties in the pelletised form, namely, pellet porosity and pellet diameter [16]. Here, we seek to investigate the influence of pellet properties towards achieving the cost limits at different CO₂ compositions. We conducted this study by comparing two optimisation cases: in the first case, pellet porosity and pellet diameter were treated as decision variables along with other adsorbent and process decision variables in the optimisations, while the second case involves keeping pellet porosity and pellet diameter as fixed values. The cost limits discussed earlier represents the first case, meanwhile unique optimisations were carried out for the second case using fixed values of pellet porosity ($\epsilon_p=0.37$) and pellet diameter ($d_p=1.5$ mm) from the previous publication [25] which represents typical experimental values [27, 31].

Figure 4(a) illustrates the comparison between the two cases. For the entire range of CO₂ compositions considered, the difference between the minimum CO₂ avoided costs for the two cases varies between 9 to 22%. At higher CO₂ compositions (i.e. $\geq 13\%$), the cost limits for fixed pellet properties are about 9-11% higher than the cost limits where pellet

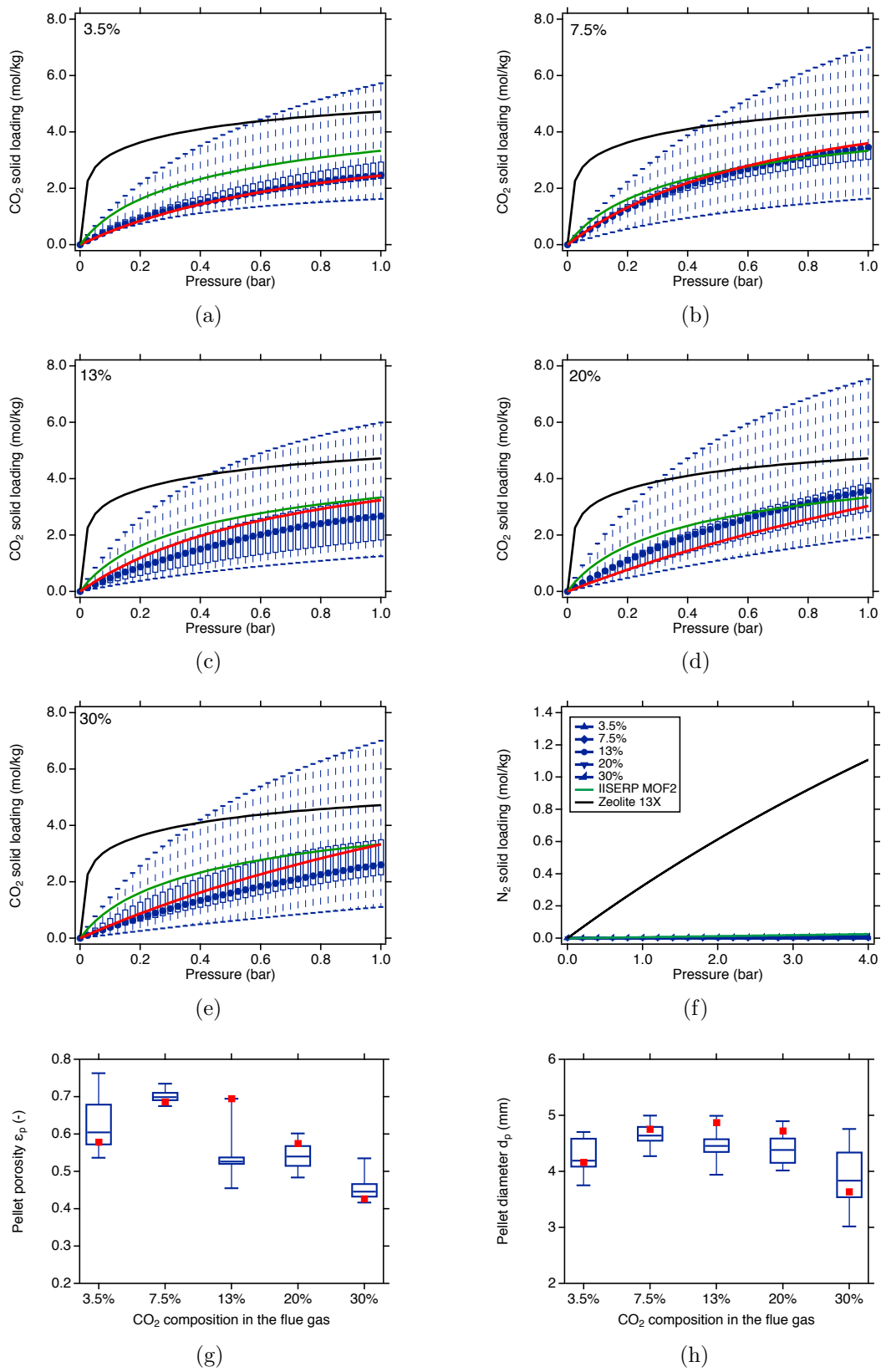


Figure 3: Optimal adsorbent properties corresponding to the cost limits of the four step PVSA cycle. (a)-(e) show the optimal CO₂ adsorption isotherms (red lines) at different CO₂ compositions. Box and whisker plots in (a)-(e) represent the range of CO₂ adsorption isotherms in the 5% vicinity of the lowest possible CO₂ avoided cost. (f) the optimal N₂ adsorption isotherms at different CO₂ compositions. For comparison, CO₂ isotherms on Zeolite 13X (black lines) and IISERP MOF2 (green lines) are also shown in (a)-(e) and (f), respectively. (g) and (h) illustrate the optimal pellet porosity and diameter (red squares) along with box and whisker plots that represent the values within the 5% vicinity of the minimum CO₂ avoided costs, respectively.

properties were varied. This difference increases to 19-22% at lower CO₂ compositions (i.e. <13%). The improvement in CO₂ avoided costs through optimisation of pellet morphology can be attributed to the increased values of optimal ϵ_p and d_p as shown in Fig. 3(g)-(h). The optimal values of ϵ_p vary between 0.42 and 0.76, whereas the optimal d_p lies in between 3.0 and 5.0 mm, which are greater than the typical pellet sizes used in PVSA operations. It is worth noting that Farmahini *et al* also report similar ranges for ϵ_p and d_p in their energy-productivity optimisations [16]. The choice of such increased values of ϵ_p and d_p by the optimiser is a result of an interplay between mass transfer characteristics and pressure drop. To elaborate, larger d_p favours lower pressure drop across the adsorption columns (see Ergun’s equation in the supporting information) and also increases the maximum feed velocity (minimum fluidisation limit) in the adsorption step. Hence, the adsorption columns can be operated at increased feed velocities with lower compression energy consumption, thereby facilitating the reduction in the number of parallel PVSA trains. Consequently, lower capital costs and compression costs are attained. Contrarily, the mass transfer is hindered by the increase in d_p , as given by the following relationship: $k_{LDF} \propto \frac{\epsilon_p}{d_p^2}$, where, k_{LDF} is the mass transfer coefficient. Keeping all other parameters constant, increase in d_p , reduces k_{LDF} which means that the mass transfer resistance is increased. This consequently increases the durations of constituent steps to meet constraints. To counter this effect, the optimiser chose high ϵ_p values to allow for enhanced mass transfer. As a result, there will be a lower amount of adsorbent present in the column, along with shorter PVSA cycle times. Shorter adsorption cycles lead to a fewer number of columns in a single PVSA train. This contributes to reducing capital costs from fewer columns and vacuum pumps needed to implement the cycle scheduling. As can be seen from Fig. 3(g), the optimal ϵ_p values have not approached the upper limit as the adsorption column requires a certain minimum amount of adsorbent in the column to meet the CO₂ purity-recovery constraints. While higher ϵ_p and d_p are preferred theoretically, practical considerations such as the mechanical stability and the ability to synthesise high porosity pellets must be considered [16].

Influence of adsorbent costs.. While an adsorbent cost of zero is interesting to understand the cost limit of PVSA, adsorbent costs cannot realistically be expected to be zero. Although the adsorbent costs are dependant on the raw materials used to synthesise them, scale-up methods, etc., the question we asked is: if hypothetical adsorbents could be synthesised at similar costs as that of commercial adsorbents, what would be their contribution in bringing down CO₂ avoided costs? Hence, we studied the influence of adsorbent costs on the cost limits by considering three different adsorbent costs: 1) zero; 2) 1500 and; 4500 € per tonne of adsorbent. To provide context, commercial adsorbent like Zeolite 13X costs about 1500 € per tonne [15, 25]. Like previous case studies, we carried out unique optimisations for each case where we minimised the CO₂ avoided cost by varying both adsorbent and process decision variables. The cost limits at zero adsorbent cost serve as a reference. As can be seen from Fig. 4(a), the adsorbent costs we considered have a marginal effect on the cost limits for all CO₂ compositions. For the case of 1500 € per tonne, the cost limits obtained are <10% higher than the cost limits with zero adsorbent cost, whereas 7-13% higher when the adsorbent costs are increased three times the cost of Zeolite 13X.

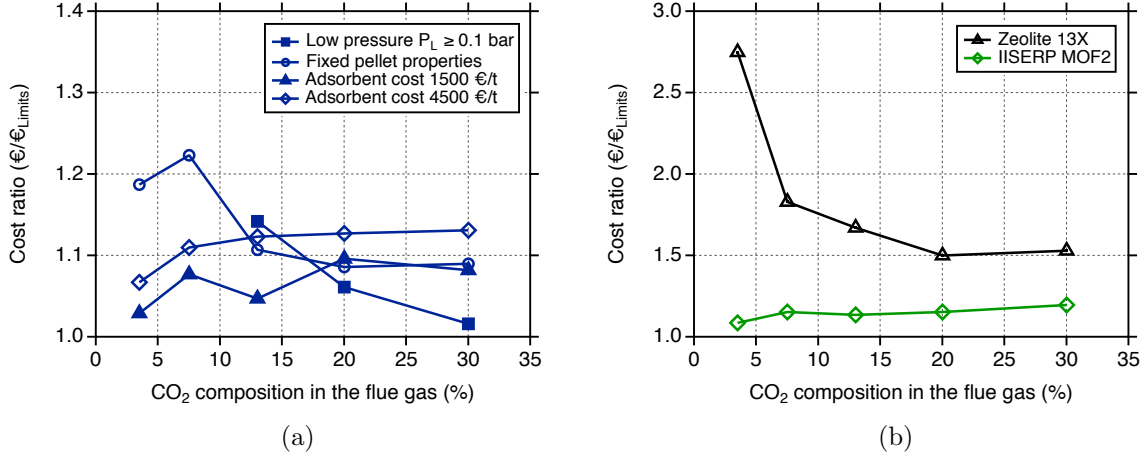


Figure 4: (a) Impact of different process parameters on the cost limits of the four-step PVSA cycle. (b) Comparison between the cost limits of the four-step PVSA cycle with minimum CO₂ avoided costs obtained for real adsorbents (Zeolite 13X and IISERP MOF2). The cost ratio was defined as the ratio between minimum CO₂ avoided costs obtained for the examined cases and the cost limits reported in Fig. 1 (a) at each CO₂ composition. Note that the absolute costs decrease with increase in CO₂ composition.

4.2. Comparison with real adsorbents

The cost limits obtained previously are compared to the performance of real adsorbents. The rationale behind this case study was to understand the performance gaps between “ideal” and “real” adsorbents, hence the theoretical room for improvement by developing novel adsorbent materials. Two real adsorbents are considered: Zeolite 13X, the current benchmark material for post-combustion CO₂ capture [29, 34] and; IISERP MOF2, a novel MOF that was found to be promising in a recent screening study [17] and in a techno-economic assessment [25]. It is worth noting that Zeolite 13X is currently deployed for industrial applications, whereas IISERP MOF2 is still in the early stages of development with synthesis at the lab scale. To determine the minimum avoided costs for Zeolite 13X and IISERP MOF2 at different CO₂ compositions in the flue gas, optimisations were carried out by varying process decision variables along with pellet porosity and pellet diameter. Since the adsorption equilibria for these adsorbents are known, adsorbent isotherm variables are held constant in these optimisations. Further, we have accounted for the adsorbent costs of 1500 and 4500 € per tonne for Zeolite 13X and IISERP MOF2, respectively [25].

Figure 4(b) shows the comparison of minimum CO₂ avoided costs obtained for Zeolite 13X (black line) and IISERP MOF2 (green line) and cost limits. Of the two “real” adsorbents, Zeolite 13X always resulted in higher CO₂ avoided costs than IISERP MOF2. At 30% CO₂ composition, the minimum CO₂ avoided cost obtained for Zeolite 13X was 18.7 € per tonne of CO₂ avoided (see Table S18 in the supporting information) which is about 53% higher than the cost limit at the same CO₂ composition. The gap monotonically increases with reducing the CO₂ composition. For instance, the difference in CO₂ avoided costs between the Zeolite 13X and the cost limits at 3.5% CO₂ composition is approximately 175%.

Higher CO₂ avoided costs for Zeolite 13X can be attributed to its non-linear CO₂ and high capacity N₂ isotherms, as shown in Fig. 3. While the band of hypothetical CO₂ isotherms from the cost limit optimisations are fairly linear, the non-linearity of the CO₂ isotherm for Zeolite 13X results in long blowdown and evacuation steps and, consequently, the capital costs [25]. On the other hand, previous studies have consistently shown that lower N₂ affinity significantly reduces electricity consumption [23, 17]. Since the Zeolite 13X higher N₂ affinity as compared to hypothetical N₂ isotherms, higher electricity costs are incurred compared to the “ideal” adsorbents (see Table S18 in the supporting information).

As can be observed from the Fig. 4(b), the marginal gap between the green line and the reference value 1.0 indicates the superior performance of IISERP MOF2, and this can be attributed to features of CO₂ and N₂ isotherms illustrated in Fig. 3. For all CO₂ compositions, the CO₂ isotherms of IISERP MOF2 are within the band of hypothetical CO₂ isotherms from the cost limits case. In addition, lower N₂ affinity similar to hypothetical N₂ isotherms contributed to lower electricity costs [25, 23]. Further when the CO₂ compositions are lowered, the difference between the minimum CO₂ avoided costs of IISERP MOF2 and the cost limits also decreases non-monotonically from 20% to 9%.

Based on these results, it can be inferred that the dual-site Langmuirian-type “real” adsorbents can achieve relatively low CO₂ avoided costs at high CO₂ compositions, while their performances are discouraging at low CO₂ compositions. Conversely, the performances obtained by IISERP MOF2, an adsorbent approaching those “ideal” features previously outlined, are consistently close to the cost limits.

4.3. Cost limits of six-step DR cycle

As discussed previously, the four-step PVSA cycle relies strongly on the deep vacuum (< 0.1 bar) to meet CO₂ purity-recovery constraints for CO₂ compositions lower than 30%. Although limiting the lower limit of P_L to 0.1 bar in the optimisations resulted in minimum CO₂ avoided costs slightly higher ($\leq 14\%$) than the cost limits for CO₂ compositions $\geq 13\%$, the CO₂ purity-recovery constraints were, however, not met for lower CO₂ compositions, i.e. $< 13\%$. Hence, we investigated a more complex six-step cycle with DR [28, 20, 21] by carrying out unique optimisations to determine if this cycle can yield lower cost limits than the four-step PVSA cycle while facilitating process operation at industrially feasible vacuum levels over a range of CO₂ compositions. Figure 1(b) shows the comparison of cost limits between the two PVSA cycles. As can be observed that the cost limits obtained for the six-step DR cycle are lower than the four-step cycle. For 30% CO₂ composition, the difference between the cost limits is 1.8 € per tonne of CO₂ avoided (i.e. $\approx 15\%$ lower for six-step DR cycle). When the CO₂ composition is lowered to 20%, the cost limits of the six-step DR cycle were found to be 24% lower than the cost limits achieved for the four-step cycle. The cost reduction ($\approx 42\%$) is more significant as the CO₂ composition is lowered from 20% to 3.5%. As can be seen from Figs. 1(d) and (f), the decrease in capital and, more significantly, operating costs have contributed to the cost reductions of the six-step DR cycle. As compared to the four-step cycle, the electricity costs have significantly dropped, especially at lower CO₂ compositions. This can be attributed to the optimal P_H and P_L

(shown in Fig. 2) required to achieve the lowest CO₂ avoided costs. Optimal P_H for the six-step DR cycle always remained lower than that of the four-step cycle over a range of CO₂ compositions which indicate lower compression costs. Another interesting aspect remains that the six-step DR cycle can be operated with $P_L \geq 0.1$ bar over the entire range of CO₂ compositions. This is a significant result because the industrially used vacuum pumps can now be employed. The ability to operate vacuum pumps at milder vacuum levels further entails lower electricity consumption, not only connected to the higher P_L but also, the higher vacuum pump efficiencies. The better performance of the six-step DR cycle over the four-step cycle can be attributed to the dual reflux steps, i.e. the HR and LR steps. The LR step in the six-step DR cycle helped recover the residual CO₂ from the column after the evacuation step, and the effluent of this step was used as the heavy reflux before the depressurisation steps. The HR step increased the overall CO₂ partial pressure in the column. Hence, the CO₂ purity-recovery targets can be achieved without depressurising the column to deep vacuum levels [28].

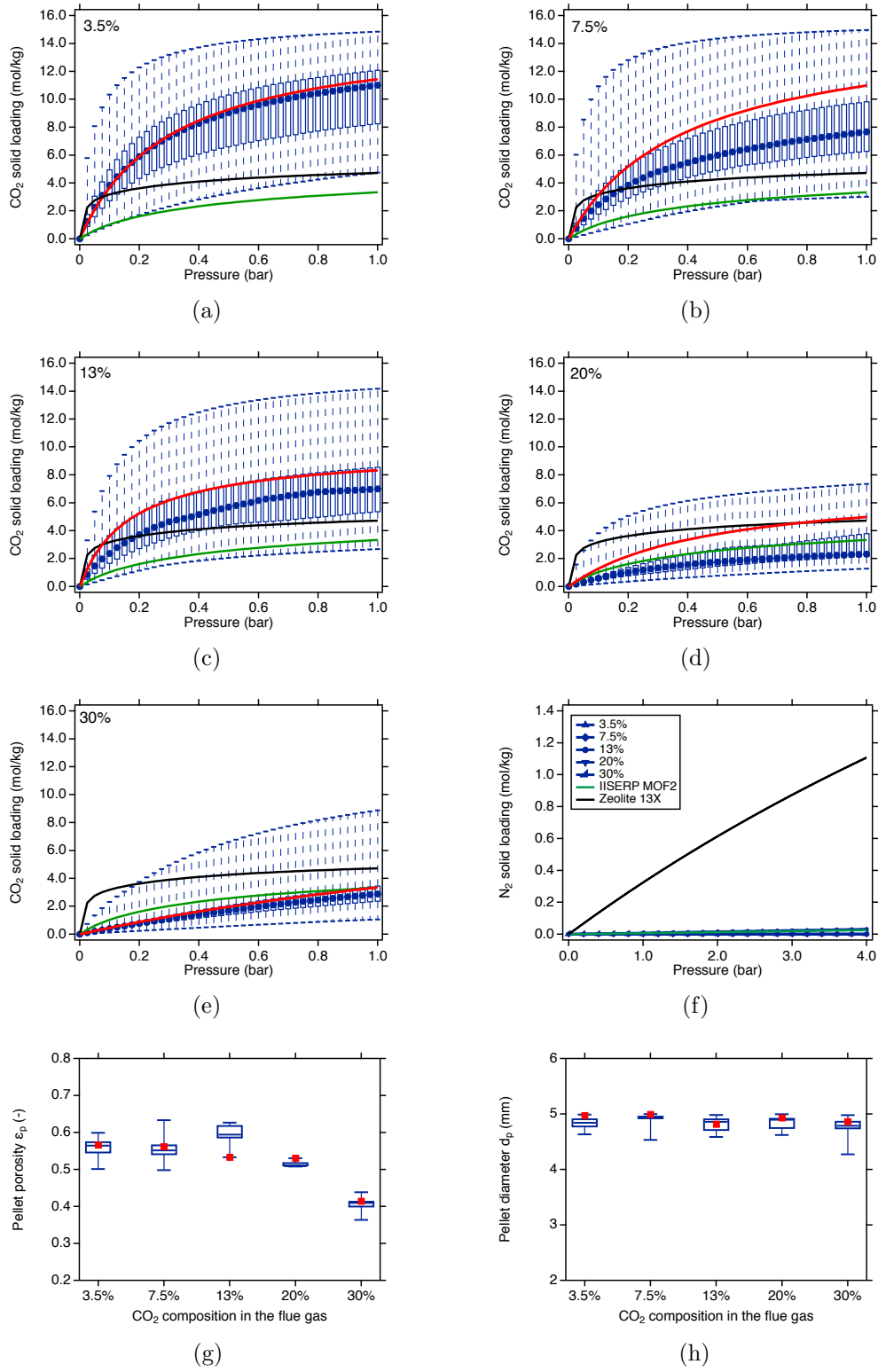


Figure 5: Optimal adsorbent properties corresponding to the cost limits of six step DR cycle. (a)-(e) show the optimal CO₂ adsorption isotherms at different CO₂ compositions. Box and whisker plots in (a)-(e) represent the range of CO₂ adsorption isotherms in the 5% vicinity of the lowest possible CO₂ avoided cost. (f) show the optimal N₂ adsorption isotherms at different CO₂ compositions. For comparison CO₂ and N₂ adsorption isotherms of Zeolite 13X (black lines) and IISERP MOF2 (green lines) are also shown in (a)-(e) and (f), respectively. (g) and (h) illustrate the optimal pellet porosity and diameter, respectively, corresponding to the cost limits of six step DR cycle.

The optimal adsorbent properties linked to the cost limits of the six-step DR cycle are shown in Fig. 5. Similar to the four-step cycle, we also noticed a huge variation of CO₂ isotherms and pellet properties within a 5% range from the minimum avoided costs for the six-step DR cycle. The CO₂ isotherms for the six-step DR cycle were also found to be fairly linear with almost zero N₂ adsorption (see Fig. 5). For CO₂ compositions of 3.5%, 7.5% and 13%, the CO₂ isotherms of the six-step DR cycle showed a huge variation with higher loadings as compared to the four-step cycle. The band of CO₂ isotherms for both the cycles were comparable for 20% and 30% CO₂ compositions. On the other hand, the pellet diameters were closer to the upper limit of 5 mm, whereas the pellet porosity lies in the range of 0.36-0.63.

4.4. Comparison with MEA absorption

Here, the competitiveness of PVSA for post-combustion CO₂ capture is analysed by comparing its cost limits with current benchmark MEA absorption. The CO₂ avoided costs for MEA obtained from two scenarios are considered: in the first scenario, the source of steam supply for MEA-based capture comes from a natural gas (NG) boiler, whereas in the second scenario, the steam is considered to be generated through heat recovery from the industrial facility. While the first scenario serves as a more general representation of standard MEA-based capture, the second scenario is highly site-specific, i.e. depends on the availability of suitable process waste heat in the industrial facility or nearby industries. The choice of these MEA scenarios comes from the fact that the source of steam supply strongly affects the overall CO₂ avoided costs obtained using the MEA solvent [5], and such variations must be considered when assessing the techno-economic performance of PVSA for a fair comparison. Figure 1 (b) compares the CO₂ avoided costs obtained using the MEA solvent from these scenarios at different CO₂ compositions for a constant flue gas flow rate of 2004 tonnes h⁻¹. The cost limits of both PVSA cycles are lower than the CO₂ avoided costs obtained for the MEA solvent with NG boiler case when CO₂ composition $\geq 7.5\%$. At 3.5% CO₂ composition, the cost limits of both PVSA cycles escalate very quickly due to significant electricity demands, thus, resulting in a poor performance as compared to the MEA absorption. Moreover, the energy consumption for the MEA with NG boiler varies from 4.9 to 4.0 GJ_{th} t_{CO₂}⁻¹ as the CO₂ composition is increased from 3.5% to 30%, which consistent with other studies reported in the literature [35]. On the other hand, the six step DR cycle shows better cost performance than the MEA solvent with process waste heat (PWH) case for CO₂ compositions $\geq 13\%$. The MEA-PWH scenario, although site-specific and subject to the availability for CO₂ capture, represents the optimistic case for the MEA. This indicates that the PVSA could potentially outperform MEA-PWH in terms of CO₂ avoided costs for all CO₂ compositions $\geq 13\%$ should the right adsorbent be deployed.

Effect of plant scale.. So far, we have considered a single flue gas flow rate of 2004 tonnes h⁻¹ in the analysis. We now examine the effect of plant size on the cost performance of the PVSA. As specified in Table 1, five different flue gas flow rates spanning the entire spectrum of various post-combustion industrial point sources are considered. The two MEA scenarios mentioned above are used for comparison. Given the inherent way in which the PVSA

operates as multiple modules, it is expected that the overall CO₂ avoided costs will not be influenced by the plant size (or flue gas flow rate). To corroborate this assumption, we carried out optimisations to determine the cost limits of the four-step PVSA cycle at different flue gas flow rates from Table 1 for a fixed CO₂ composition of 20%. We present the results in Fig. S7 in the supporting information. As expected, the minimum CO₂ avoided costs obtained at different flue gas flow rates from unique optimisations are almost identical (<2% difference). Based on these results, we extended the same values of the cost limits obtained for both PVSA cycles in Fig.1(b) at different CO₂ compositions over a range of flue gas flow rates considered without re-running the optimisations for each case. Figure 6 illustrates the impact of both plant size and CO₂ composition on the overall competitiveness of the PVSA. We considered the six-step DR cycle as the representative case for PVSA owing to its superior performance. The red-shaded portions of the figure indicate better performance of MEA over PVSA, while the blue-shaded portions show the superior performance of PVSA over MEA. The text in each box represents the percentage by which the CO₂ avoided costs of PVSA are higher/lower compared to the MEA. A (+) sign indicates that the PVSA costs are higher than the MEA and a (-) indicates that the PVSA costs are lower than the MEA. For the MEA-NG case as reference, the PVSA outperforms MEA for all flue gas flow rates and with CO₂ composition >3.5%. Notably, one exception was found where the PVSA performs slightly better than MEA for a flue gas flow rate of 313 tonne h⁻¹ at 3.5% CO₂ composition. When MEA-PWH is considered as the basis, the PVSA results in lower costs for all flue gas flow rates with CO₂ composition ≥13%. These results indicate that the PVSA has a cost advantage compared to the benchmark MEA solvent for CO₂ compositions ≥13% over a range of flue gas flow rates provided low-cost adsorbents with appropriate separation capabilities can be developed.

Complexity of the PVSA plant.. One of the challenges of the implementation of the PVSA involves integrating multiple PVSA trains. Depending on the plant size and the CO₂ composition, several PVSA trains might be needed for operation. We present the required number of PVSA trains for both four-step cycle and six-step DR cycle in order to treat 2004 tonne h⁻¹ flue gas flow rate in Fig. 7(a). In addition, the range within the 5% vicinity of cost limits is also shown. As can be seen from the figure, the overall trend, considering also the ranges for the 5% vicinity, is that both the number of trains and the column footprint remains fairly constant. This trend is consistent as the amount of flue gas to be treated remains the same, immaterial of the CO₂ composition. The required number of PVSA trains for a fixed CO₂ composition linearly increases with the flue gas flow rates as shown in Fig. 7(b) (also see Table S21 in the supporting information). For instance, 8 PVSA trains are needed to treat 313 tonne h⁻¹ of flue gas at 20% CO₂ composition. On the contrary, 79 PVSA trains are required if the flow rate increases to 3696 tonne h⁻¹. Moreover, we illustrate the footprint of the columns when stacked side by side for the case of the 2004 tonne h⁻¹ flow rate in Fig. 7(a). As can be seen from the figure, the column footprint ranges between ≈1000-2200 m². Over a range of flue gas flow rates at 20% CO₂ composition, the column footprint, as illustrated in Fig. 7(b), varies almost linearly from 209 m² to 2234 m² when the flow rate changes from 313 to 3696 tonne h⁻¹, respectively. It is to be noted that the

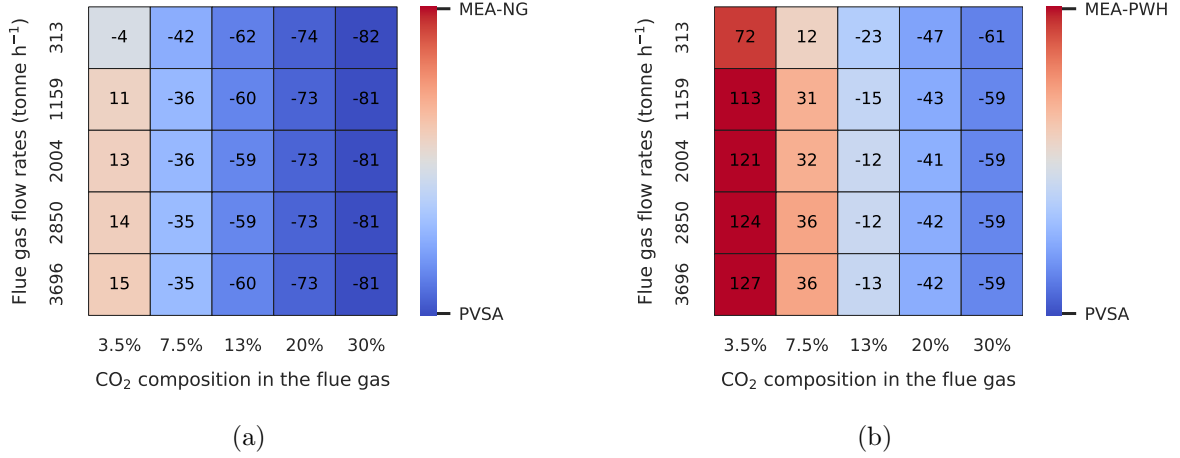


Figure 6: Heat maps illustrating the cost performance of the six-step DR PVSA cycle as compared to standard (a) MEA solvent using natural gas (NG) for steam generation (b) MEA solvent using process waste heat (PWH) for steam generation. The red-shaded portions indicate that the CO₂ avoided costs of PVSA are higher than that of MEA while the blue-shaded portions indicate that the CO₂ avoided costs of PVSA are lower than the MEA. The text in the heat maps represents the percentage by which the CO₂ avoided costs of PVSA are higher/lower compared to the MEA. A (+) sign indicates that the PVSA costs are higher than the MEA and a (-) indicates that the PVSA costs are lower than the MEA.

total footprint of the plant will be higher than the values reported after adding the area occupied by compressors, vacuum pumps and piping.

Electricity scenarios. As previously described, the electricity demand remains the significant factor towards achieving the minimum CO₂ avoided costs for PVSA. In this study, we used the standard European electricity price of 58.1 € per MWh [25, 36]. For the electricity consumed, we also accounted for the specific direct emissions of 38 kg CO₂ per MWh based on the assumption that the electricity consumed by the PVSA is supplied through a deeply decarbonised power system based on a fossil-based power plant with CCS and renewables [25]. As indirect CO₂ emissions associated with electricity consumption increase the CO₂ avoidance cost [37], the premise of a deeply decarbonised power system is consistent with the search for the cost limit. Since the source of electricity generation and its characteristics depends on several parameters such as plant location and electricity mix, we conducted an optimisation study with alternative scenarios to investigate the impact on PVSA cost limits. For this analysis, the electricity price of 58.1 € per MWh and the specific direct emissions of 38 kg CO₂ per MWh remain as the base case. In Scenario 1, we reduced the cost of electricity to 50% of the base case while the specific direct emissions were kept the same as the base case. This scenario is representative of cases in which the PVSA facilities access low-cost renewable electricity production with preferential industrial tariffs excluding transmission costs as can happen, for example, in Norway [38]. Scenario 2 considers the electricity generation with higher CO₂ intensity, i.e., the cost of electricity remains the same

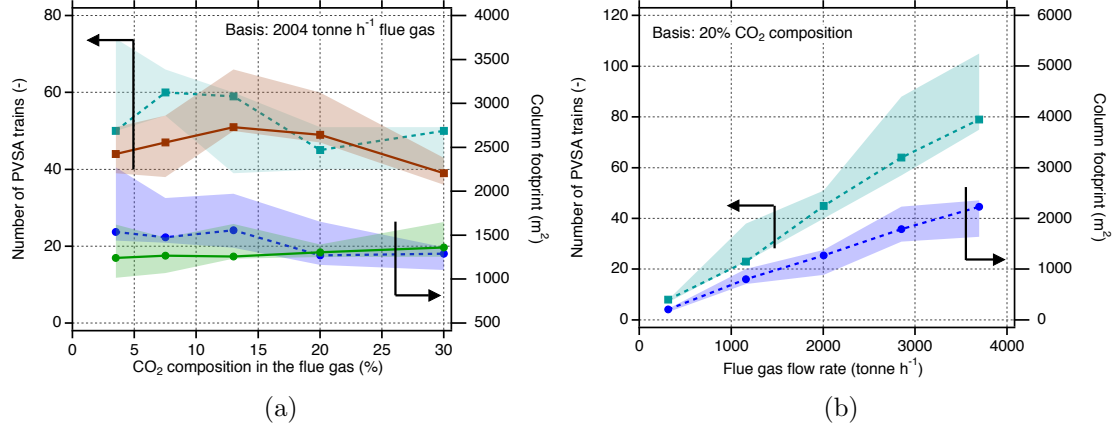


Figure 7: PVSA trains (squares) and column footprint (circles) required to treat (a) 2004 tonne h⁻¹ flue gas at different CO₂ compositions based on the cost limits of four-step (dashed lines) and six-step DR (solid lines) cycles (b) different flue gas flow rates at 20% CO₂ composition based on the cost limits of four-step cycle. Shaded region represents the range within the 5% vicinity of the lowest possible CO₂ avoided costs.

as that of the base case while the specific direct emissions are increased to 262 kg CO₂ per MWh corresponding to the CO₂-intensity of the European average electricity mix [36, 39]. The motivation for the second scenario comes from the existing power production systems that are significantly based on fossil-fuel power plants without CCS.

We optimised the PVSA cost limits based on the two alternative electricity scenarios. Figure 8 illustrates the cost limits obtained for two PVSA cycles under the two alternative scenarios. As can be seen from the figure, the cost limits of both PVSA cycles are lowered ($\approx 23\text{--}32\%$) when the electricity prices dropped to 29.0 € per MWh in Scenario 1. Under these circumstances, the six-step DR cycle outperforms MEA with NG boiler for all CO₂ compositions, whereas the four-step cycle gives lower costs for CO₂ compositions $\geq 7.5\%$. If MEA-PWH is considered as reference, then the six-step DR and four-step cycles perform better than MEA for CO₂ compositions $\geq 7.5\%$ and $\geq 13\%$, respectively. On the contrary, the PVSA cost limits have either increased or remained the same when Scenario 2 is considered. The high CO₂ intensity in Scenario 2 showed a substantial effect on two PVSA cycles at a 3.5% CO₂ composition where the CO₂ avoided cost increased to 246.4 € per tonne of CO₂ avoided (64% higher than the base case) for the four-step cycle. When the six-step DR cycle is considered, the CO₂ avoided cost increased to 105.1 € per tonne of CO₂ avoided, i.e. almost 21% higher than the base case. This is because the electricity consumption is significantly higher at 3.5% CO₂ composition (see Fig. 1(c)-(d)) than other higher CO₂ compositions. The four-step cycle, however, obtained 68.4 € per tonne of CO₂ avoided, i.e. 17% higher costs compared to the base case at 7.5% CO₂ composition. For CO₂ compositions $\geq 13\%$, the CO₂ intensity has negligible effect on the PVSA cost limits.

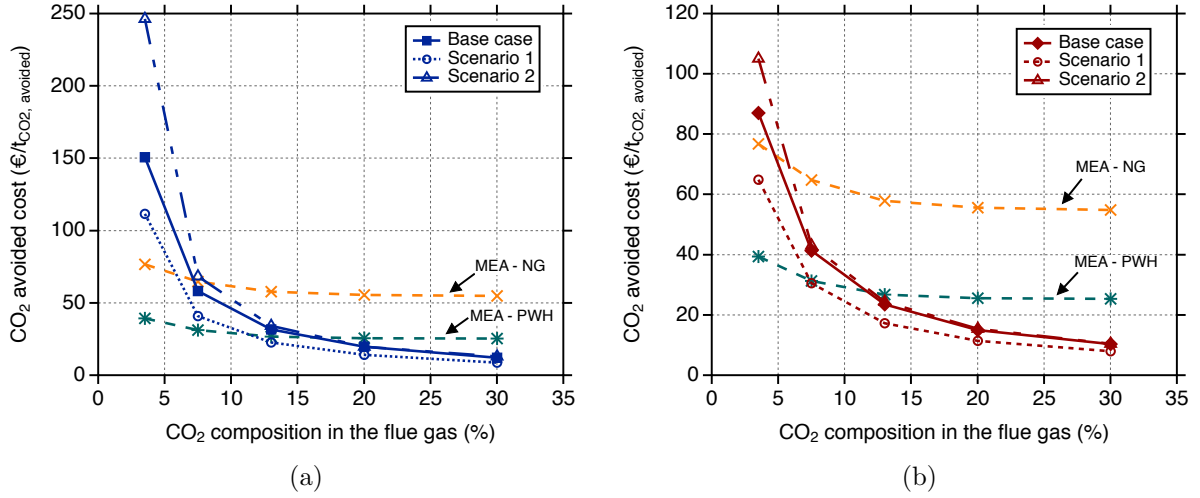


Figure 8: Cost limits of (a) four-step and (b) six-step DR PVSA cycles when two alternative electricity scenarios are considered: Scenario 1 - electricity price of 29.0 € per MWh and specific direct emissions of 38 kg CO₂ per MWh and; Scenario 2 - electricity price of 58.1 € per MWh and specific direct emissions of 262 kg CO₂ per MWh. The base case with the cost of electricity 58.1 € per MWh and specific direct emissions of 38 kg CO₂ per MWh also shown corresponds to the cost limits reported in Fig. 1(b).

5. Conclusions

Cost limits of two single-stage PVSA cycles for post-combustion CO₂ capture are investigated through techno-economic optimisations based on a *process inversion* approach. Using this approach, both adsorbent and process variables are simultaneously optimised based on NSGA-II algorithm to calculate the lowest possible cost of CO₂ avoided (excluding the costs of CO₂ conditioning, transport and storage) or cost limits at different flue gas flow rates and CO₂ compositions. The key results of this study can be summarised as follows:

- We showed that the CO₂ composition in the flue gas significantly impacts the cost limits of PVSA, i.e., the lowest possible CO₂ avoided costs decrease with increase in CO₂ compositions. Between the two cycles considered, the six-step DR cycle achieved 15-42% lower costs compared to the four-step cycle, depending on the CO₂ composition.
- When compared with the established MEA solvent based on NG boiler as a steam source, the four-step PVSA cycle has at least 8% lower costs compared to the MEA-based CO₂ capture, whereas the six-step DR PVSA cycle has at least 35% lower costs for CO₂ compositions $\geq 7.5\%$ over a range of flue gas flow rates.
- The optimisations indicated that the “ideal” adsorbents that facilitate lowest possible CO₂ avoided costs have fairly linear CO₂ adsorption isotherms and N₂ adsorption close to zero.

- It was found that modifying the pellet morphology can result in $\approx 9\text{-}22\%$ lower CO₂ avoided costs based on a four-step PVSA cycle. The optimal pellet porosities and diameters were between 0.42-0.76 and 3-5 mm, respectively.
- The complexity of the PVSA plant in terms of the number of trains, equipment, piping, area, etc., significantly depends on the flue gas flow rate. The smallest plant considered in this study with a size of 313 tonne h⁻¹ flue gas flow rate requires about eight PVSA trains with four columns each based on a four-step PVSA cycle. Almost 79 PVSA trains with four columns each are needed to treat a plant size of 3696 tonne h⁻¹.

Although the PVSA costs seem favourable, the practical implementation involves limitations due to the plant complexity in terms of the number of PVSA trains required to treat the flue gas, the footprint of the total plant and the associated complexities in plant integration. Some of the challenges can be offset by choosing horizontally-oriented columns, or radial-flow columns, instead of the vertically-oriented columns, and by potentially considering hybrid processes, e.g., PVSA+cryogenic [40, 41]. Future work should also focus on the use of structured adsorbents that can provide faster mass transfer rates combined with lower pressure drops. It is worth emphasizing that with the impetus on reaching net-zero emissions by 2050, technologies and the economics will continue to evolve. The framework provided in this work could serve as the basis for the evaluation of PVSA processes in the future. Finally, the key outcome of the study is the demonstration that PVSA processes can be promising for treating flue gas streams with high CO₂ compositions, provided suitable low-cost adsorbents be developed. The fact that adsorbents with a variety of CO₂ isotherms can indeed yield similar costs is encouraging and provides the motivation of adsorbent discovery and development.

Author Contributions

Sai Gokul Subraveti: Conceptualization, Methodology, Software, Formal Analysis, Writing-Original Draft, Writing- Review and Editing; **Simon Roussanaly:** Conceptualization, Methodology, Software, Formal Analysis, Writing- Review and Editing, Supervision, Funding acquisition; **Rahul Anantharaman:** Conceptualization, Methodology, Writing-Review and Editing; **Luca Riboldi:** Conceptualization, Methodology, Writing- Review and Editing; **Arvind Rajendran:** Conceptualization, Methodology, Writing- Review and Editing, Supervision, Funding acquisition

Conflicts of interest

There are no conflicts to declare.

Acknowledgements

The authors acknowledge the financial support from Canada First Excellence Fund through the University of Alberta's Future Energy Systems and Norwegian Carbon Capture and Storage (NCCS) Centre performed under the Norwegian research program Centres

for Environment-friendly Energy Research (FME). The authors acknowledge the following partners for their contributions: Aker Solutions, Ansaldo Energia, Baker Hughes, CoorsTek Membrane Sciences, EMGS, Equinor, Gassco, Krohne, Larvik Shipping, Lundin, Norcem, Norwegian Oil and Gas, Quad Geometrics, Total, Var Energi, and the Research Council of Norway (257579/E20). Compute Canada provided the computational resources.

Electronic Supplementary Information

Details corresponding to the following aspects are provided: PVSA plant layout; cost performance of MEA-based CO₂ capture; techno-economic modelling framework; dual-site Langmuir isotherm parameters for the two adsorbents; two PVSA cycles and their modelling; PVSA simulation parameters; cost model and cycle scheduling; technical modelling of compressors, vacuum pumps and heat exchangers; optimisation decision variable bounds; optimal decision variables along with the breakdown of capital and operating costs for the optimisations considered. Figures related to: optimal adsorbent properties obtained for the six-step DR cycle, optimal cycle scheduling, and the effect of plant size on PVSA costs are also illustrated.

- [1] IPCC, “Global warming of 1.5°C. an ipcc special report on the impacts of global warming of 1.5°C above pre-industrial levels and related global greenhouse gas emission pathways, in the context of strengthening the global response to the threat of climate change, sustainable development, and efforts to eradicate poverty,” 2018.
- [2] IEA, “Transforming industry through CCUS, IEA, Paris,” 2019.
- [3] IPCC, “Ipcc special report on carbon dioxide capture and storage. prepared by working group iii of the intergovernmental panel on climate change,” 2005.
- [4] A. H. Farmahini, S. Krishnamurthy, D. Friedrich, S. Brandani, and L. Sarkisov, “Performance-based screening of porous materials for carbon capture,” *Chem. Rev.*, vol. 121, pp. 10666–10741, 2021.
- [5] C. Fu, D. Kim, S. Roussanaly, S. Gardarsdottir, and R. Anantharaman, “Post-combustion CO₂ capture using MEA – benchmarking performance and insights for a wide range of industrially relevant scenarios,” *To be submitted to Energies*.
- [6] M. Bui, C. S. Adjiman, A. Bardow, E. J. Anthony, A. Boston, S. Brown, P. S. Fennell, S. Fuss, A. Galindo, L. A. Hackett, J. P. Hallett, H. J. Herzog, G. Jackson, J. Kemper, S. Krevor, G. C. Maitland, M. Matuszewski, I. S. Metcalfe, C. Petit, G. Puxty, J. Reimer, D. M. Reiner, E. S. Rubin, S. A. Scott, N. Shah, B. Smit, J. P. M. Trusler, P. Webley, J. Wilcox, and N. Mac Dowell, “Carbon capture and storage (CCS): the way forward,” *Energy Environ. Sci.*, vol. 11, pp. 1062–1176, 2018.
- [7] L.-C. Lin, A. H. Berger, R. L. Martin, J. Kim, J. A. Swisher, K. Jariwala, C. H. Rycroft, A. S. Bhowan, M. W. Deem, M. Haranczyk, and B. Smit, “In silico screening of carbon-capture materials,” *Nat. Mater.*, vol. 11, p. 633–641, 2012.
- [8] C. E. Wilmer, O. K. Farha, Y.-S. Bae, J. T. Hupp, and R. Q. Snurr, “Structure–property relationships of porous materials for carbon dioxide separation and capture,” *Energy Environ. Sci.*, vol. 5, pp. 9849–9856, 2012.
- [9] J. M. Huck, L.-C. Lin, A. H. Berger, M. N. Shahrak, R. L. Martin, A. S. Bhowan, M. Haranczyk, K. Reuter, and B. Smit, “Evaluating different classes of porous materials for carbon capture,” *Energy Environ. Sci.*, vol. 7, pp. 4132–4146, 2014.
- [10] M. Khurana and S. Farooq, “Adsorbent screening for postcombustion CO₂ capture: A method relating equilibrium isotherm characteristics to an optimum vacuum swing adsorption process performance,” *Ind. Eng. Chem. Res.*, vol. 55, no. 8, pp. 2447–2460, 2016.

- [11] J. Park, R. P. Lively, and D. S. Sholl, "Establishing upper bounds on CO₂ swing capacity in sub-ambient pressure swing adsorption via molecular simulation of metal-organic frameworks," *J. Mater. Chem. A*, vol. 5, pp. 12258–12265, 2017.
- [12] A. K. Rajagopalan, A. M. Avila, and A. Rajendran, "Do adsorbent screening metrics predict process performance? a process optimisation based study for post-combustion capture of CO₂," *Int. J. Greenh. Gas Control*, vol. 46, pp. 76 – 85, 2016.
- [13] K. T. Leperi, Y. G. Chung, F. You, and R. Q. Snurr, "Development of a general evaluation metric for rapid screening of adsorbent materials for postcombustion CO₂ capture," *ACS Sustain. Chem. Eng.*, vol. 7, no. 13, pp. 11529–11539, 2019.
- [14] V. Subramanian Balashankar and A. Rajendran, "Process optimization-based screening of zeolites for post-combustion CO₂ capture by vacuum swing adsorption," *ACS Sustain. Chem. Eng.*, vol. 7, no. 21, pp. 17747–17755, 2019.
- [15] D. Danaci, M. Bui, N. Mac Dowell, and C. Petit, "Exploring the limits of adsorption-based CO₂ capture using MOFs with PVSA – from molecular design to process economics," *Mol. Syst. Des. Eng.*, vol. 5, pp. 212–231, 2020.
- [16] A. H. Farmahini, D. Friedrich, S. Brandani, and L. Sarkisov, "Exploring new sources of efficiency in process-driven materials screening for post-combustion carbon capture," *Energy Environ. Sci.*, vol. 13, pp. 1018–1037, 2020.
- [17] T. D. Burns, K. N. Pai, S. G. Subraveti, S. P. Collins, M. Krykunov, A. Rajendran, and T. K. Woo, "Prediction of MOF performance in vacuum swing adsorption systems for postcombustion CO₂ capture based on integrated molecular simulations, process optimizations, and machine learning models," *Environ. Sci. Technol.*, vol. 54, no. 7, pp. 4536–4544, 2020.
- [18] A. H. Farmahini, S. Krishnamurthy, D. Friedrich, S. Brandani, and L. Sarkisov, "From crystal to adsorption column: Challenges in multiscale computational screening of materials for adsorption separation processes," *Ind. Eng. Chem. Res.*, vol. 57, no. 45, pp. 15491–15511, 2018.
- [19] J. Park, H. O. Rubiera Landa, Y. Kawajiri, M. J. Realff, R. P. Lively, and D. S. Sholl, "How well do approximate models of adsorption-based CO₂ capture processes predict results of detailed process models?," *Ind. Eng. Chem. Res.*, vol. 59, no. 15, pp. 7097–7108, 2020.
- [20] M. Khurana and S. Farooq, "Integrated adsorbent-process optimization for carbon capture and concentration using vacuum swing adsorption cycles," *AIChE J.*, vol. 63, no. 7, pp. 2987–2995, 2017.
- [21] M. Khurana and S. Farooq, "Integrated adsorbent process optimization for minimum cost of electricity including carbon capture by a VSA process," *AIChE J.*, vol. 65, no. 1, pp. 184–195, 2019.
- [22] B. J. Maring and P. A. Webley, "A new simplified pressure/vacuum swing adsorption model for rapid adsorbent screening for CO₂ capture applications," *Int. J. Greenh. Gas Control*, vol. 15, pp. 16 – 31, 2013.
- [23] A. K. Rajagopalan and A. Rajendran, "The effect of nitrogen adsorption on vacuum swing adsorption based post-combustion CO₂ capture," *Int. J. Greenh. Gas Control*, vol. 78, pp. 437 – 447, 2018.
- [24] K. N. Pai, V. Prasad, and A. Rajendran, "Practically achievable process performance limits for pressure-vacuum swing adsorption-based post-combustion CO₂ capture," *ACS Sustain. Chem. Eng.*, vol. 9, no. 10, pp. 3838–3849, 2021.
- [25] S. G. Subraveti, S. Roussanaly, R. Anantharaman, L. Riboldi, and A. Rajendran, "Techno-economic assessment of optimised vacuum swing adsorption for post-combustion CO₂ capture from steam-methane reformer flue gas," *Sep. Purif. Technol.*, vol. 256, p. 117832, 2021.
- [26] J. A. Ritter, S. J. Bhadra, and A. D. Ebner, "On the use of the dual-process langmuir model for correlating unary equilibria and predicting mixed-gas adsorption equilibria," *Langmuir*, vol. 27, no. 8, pp. 4700–4712, 2011.
- [27] S. Krishnamurthy, V. R. Rao, S. Guntuka, P. Sharratt, R. Haghpanah, A. Rajendran, M. Amanullah, I. A. Karimi, and S. Farooq, "CO₂ capture from dry flue gas by vacuum swing adsorption: A pilot plant study," *AIChE J.*, vol. 60, no. 5, pp. 1830–1842, 2014.
- [28] M. Khurana and S. Farooq, "Simulation and optimization of a 6-step dual-reflux VSA cycle for post-combustion CO₂ capture," *Chem. Eng. Sci.*, vol. 152, pp. 507–515, 2016.

- [29] R. Haghpanah, A. Majumder, R. Nilam, A. Rajendran, S. Farooq, I. A. Karimi, and M. Amanullah, "Multiobjective optimization of a four-step adsorption process for postcombustion CO₂ capture via finite volume simulation," *Ind. Eng. Chem. Res.*, vol. 52, no. 11, pp. 4249–4265, 2013.
- [30] M. Hosea and L. Shampine, "Analysis and implementation of TR-BDF2," *Appl. Numer. Math.*, vol. 20, no. 1, pp. 21–37, 1996.
- [31] L. Estupiñan Perez, P. Sarkar, and A. Rajendran, "Experimental validation of multi-objective optimization techniques for design of vacuum swing adsorption processes," *Sep. Purif. Technol.*, vol. 224, pp. 553 – 563, 2019.
- [32] S. Roussanaly, E. S. Rubin, M. van der Spek, G. Booras, N. Berghout, T. Fout, M. Garcia, S. Gardarsdottir, V. N. Kunchekanna, M. Matuszewski, S. McCoy, J. Morgan, S. M. Nazir, and A. Ramirez, "Towards improved guidelines for cost evaluation of carbon capture and storage," Mar. 2021.
- [33] D. Danaci, P. A. Webley, and C. Petit, "Guidelines for techno-economic analysis of adsorption processes," *Front. Chem. Eng.*, vol. 2, p. 30, 2021.
- [34] P. Xiao, J. Zhang, P. Webley, G. Li, R. Singh, and R. Todd, "Capture of CO₂ from flue gas streams with zeolite 13x by vacuum-pressure swing adsorption," *Adsorption*, vol. 14, pp. 575–582, 2008.
- [35] D. Danaci, M. Bui, C. Petit, and N. Mac Dowell, "En route to zero emissions for power and industry with amine-based post-combustion capture," *Environ. Sci. Technol.*, vol. 55, no. 15, pp. 10619–10632, 2021.
- [36] M. Voldsund, S. O. Gardarsdottir, E. De Lena, J.-F. Pérez-Calvo, A. Jamali, D. Berstad, C. Fu, M. Romano, S. Roussanaly, R. Anantharaman, H. Hoppe, D. Sutter, M. Mazzotti, M. Gazzani, G. Cinti, and K. Jordal, "Comparison of technologies for CO₂ capture from cement production—part 1: Technical evaluation," *Energies*, vol. 12, p. 559, 2019.
- [37] S. Roussanaly, N. Berghout, T. Fout, M. Garcia, S. Gardarsdottir, S. M. Nazir, A. Ramirez, and E. S. Rubin, "Towards improved cost evaluation of carbon capture and storage from industry," *Int. J. Greenh. Gas Control*, vol. 106, p. 103263, 2021.
- [38] J. Jakobsen, S. Roussanaly, and R. Anantharaman, "A techno-economic case study of CO₂ capture, transport and storage chain from a cement plant in norway," *J. Clean. Prod.*, vol. 144, pp. 523–539, 2017.
- [39] S. O. Gardarsdottir, E. De Lena, M. Romano, S. Roussanaly, M. Voldsund, J.-F. Pérez-Calvo, D. Berstad, C. Fu, R. Anantharaman, D. Sutter, M. Gazzani, M. Mazzotti, and G. Cinti, "Comparison of technologies for CO₂ capture from cement production—part 2: Cost analysis," *Energies*, vol. 12, no. 3, p. 542, 2019.
- [40] A. Wright. Personal Communication.
- [41] A. Wright, "Integrating oxyfuel CO₂ purification technologies with a post-combustion capture adsorption unit," 03 2017.